Measurement of the effect of pretreatment and adsorption on the electrical properties of ZnO powders using a microwave-Hall-effect technique

Byung-Ki Na and M. Albert Vannice*
Department of Chemical Engineering, The Pennsylvania State University, University Park, Pennsylvania 16802

Arden B. Walters
Florida Power and Light Company, P.O. Box 078768, West Palm Beach, Florida 33407-0768
(Received 27 January 1992)

Microwave-Hall-effect (MHE) and electrical conductivity measurement techniques can now be used to obtain absolute values of the electrical properties of semiconductor powders under different controlled conditions. A commercial ESR spectrometer was modified to conduct MHE experiments and a network analyzer was utilized to tune the microwave cavity and obtain Q factors. A sample of ultrahigh-purity ZnO powder (30 m^2/g) was prepared and studied. Evacuation of ZnO at 673 K decreased the electron Hall mobility but increased the conductivity and electron density at 300 K, and typical values for this high-surface-area powder were $\mu=4$ $cm^2/V\,s$, $\sigma=0.05$ $\Omega^{-1}cm^{-1}$, and $N_e=2\times10^{16}$ e^-/g. Oxygen chemisorption at 300 K increased the mobility but decreased the conductivity and electron density, and after this step typical values were $\mu=50$ $cm^2/V\,s$, $\sigma=0.001$ $\Omega^{-1}cm^{-1}$, and $N_e=2\times10^{13}$ e^-/g. These changes were reversible. The μ values varied more than an order of magnitude; therefore, the assumption of constant mobilities cannot be made safely even at these low carrier densities. Three different ZnO powders were studied to observe the effect of surface area (i.e., particle size) on electrical properties. Lattice scattering was the dominant mechanism determining electron mobility for large particles, where the particle radius was much greater than the electron mean free path; however, as the ZnO particle size approached that of the estimated electron mean free path, defect scattering in the surface region became the dominant controlling mechanism. On an evacuated ZnO surface, CO_2 adsorption had a significant effect on the electrical properties while CO adsorption had little effect, whereas on an O-covered ZnO surface CO adsorption had a noticeable effect but CO_2 adsorption produced a much smaller change. Hydrogen adsorption on either surface gave little change in electrical properties.

INTRODUCTION

A small number of efforts have been made to measure the electrical properties of certain powder samples to better understand the role of catalyst charge carriers (electrons and holes) in certain heterogeneous reactions. Conventional methods of measuring mobility and conductivity use dc or low-frequency ac currents applied to a sample compressed between two metal plates;[1-3] however, it was recognized early that dc electrical property measurements are complicated by induced metal contact electrode voltages and by the presence of grain boundaries and particle-particle contacts in powder samples. The ac-Hall-effect technique was developed in an attempt to overcome the intergrain and interparticle charge-transfer problems and allow a more accurate measurement of the mobility and absolute number of charge carriers.[4,5] Unfortunately, the accuracy of this method is also suspect because metal electrode contacts were still required and because the ac frequencies used were still much too low to prevent charge transfer across grain boundaries and particle-particle contacts for the high-surface-area materials of catalytic interest.[6] Consequently, most researchers have restricted themselves to the measurement of changes in electrical behavior because accurate electrical property values could not be guaranteed.

However, these difficulties can be circumvented by using a microwave-Hall-effect (MHE) technique for mobility combined with microwave absorption measurements for conductivity. This approach provides quantitative bulk electrical property measurements of high-surface-area powder samples because microwave cavities eliminate the need for electrode contacts and because the x-band microwave frequency is high enough to essentially eliminate charge transfer across grain boundaries and particle-particle contacts. The MHE technique has been used to measure the charge-carrier mobilities of powder samples of semiconductors and biological materials,[7-13] and it offers the potential to provide these values for dispersed metal particles.[14,15] The MHE technique developed in this laboratory involved the design and construction of new bimodal cavities for use with a slightly modified x-band Bruker electron-spin-resonance (ESR) spectrometer.[14,15] The electrical conductivities of many materials can be measured in these same cavities by an x-band microwave absorption technique utilizing a network analyzer.[15,16] The charge-carrier density is calculated from the measured mobility and conductivity values.

In this study zinc oxide was selected as a model powder sample because its electrical properties are known to change with pretreatment and cyclic adsorption and/or desorption. ZnO is an n-type semiconductor and its elec-

trical properties are dependent upon the nonstoichiometry of the lattice, which is typically oxygen deficient and can be altered by both thermal pretreatment and exposure to oxygen. It is already known that conductivity increases as ZnO is heated in vacuum and it decreases after exposure to oxygen.[1-3] Furthermore, ZnO samples with high surface-to-volume ratios might be expected to exhibit significant changes in conductivity as gases are chemisorbed on their surfaces. ZnO is of additional interest because it was an early catalyst for methanol synthesis and is still used in Cu/ZnO methanol synthesis catalysts,[17] and it has also been used for CO oxidation.[1,4,18,19] Consequently, the adsorption of O_2, CO, H_2, and CO_2 on ZnO was measured and the influence of these gases on the electrical properties of a high-surface-area zinc oxide was determined. For comparison, some dc conductivity data are available for both ZnO single crystals and powders, although the data for the latter represent relative changes rather than absolute values. The only MHE charge-carrier-mobility data reported for ZnO powder did not include variations in surface treatment.[7] This study presents MHE mobility measurements for zinc oxide under controlled environments on samples connected to an UHV adsorption system.

EXPERIMENT

x-band microwave frequencies were used to measure Hall mobilities and conductivities by slightly modifying an ESR spectrometer (Bruker ER 200D); the ESR capability was fully retained. A new MHE bimodal cavity was constructed from free-cutting brass to replace the ESR cavity. The differences in the MHE and ESR cavities are the sample location, which is at the H-field antinode in an ESR cavity and at the E-field antinode in an MHE cavity, and the two microwave connections required for the dual-mode MHE cavity. Also, for the MHE measurements, source modulation with a PIN modulator (H-P 8734B) was used instead of magnetic-field modulation. Instrument settings on the Bruker ESR console for the MHE measurements were microwave power=5.0 mW, modulation frequency=100 kHz, modulation amplitude=1.0 G, receiver gain=5×10^4, and dc magnetic field=5000 G. The Hall signal intensity was obtained from the analog output of the ESR bridge detector. A network analyzer (H-P 8720) was used to tune the bimodal cavity and to obtain Q factors and resonance frequencies. A diagram of the system is illustrated in Fig. 1, and details of the modification have been provided elsewhere.[14,15]

The sample tube for the MHE and microwave absorption measurements was made from a 5-mm outside-diameter quartz tube (Wilmad, 703-PQ) and a high vacuum valve (Ace Glass, 8195-45), as shown in Fig. 2. A quartz disk was located at the middle of the tube to support the powder sample, which was typically less than 10 mg. After evacuation the sample was cooled to room temperature and the Ace vacuum valve was closed. The sample tube was then placed in the MHE cavity and reconnected to the vacuum line. Gas adsorption and evacuation at 300 K were performed without altering the

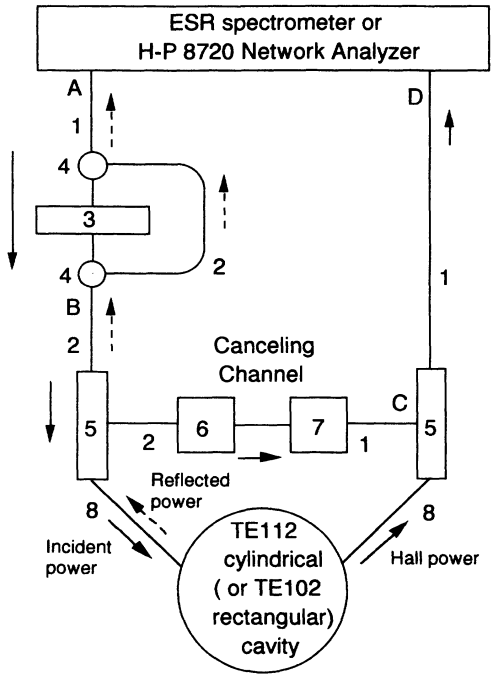

FIG. 1. Schematic of the microwave-Hall-effect system. 1, 180-cm coaxial cable; 2, 60-cm coaxial cable; 3, PIN modulator; 4, circulator; 5, 10-dB directional coupler; 6, coaxial attenuator; 7, coaxial phase shifter; 8, waveguide; A,B,C,D, connections for different experiments; arrows, microwave path.

sample position inside the cavity, thus minimizing any error due to changes in the sample position. The Q factors and resonance frequencies needed for the microwave conductivity calculations were obtained during the cavity tuning procedure prior to the MHE measurements.

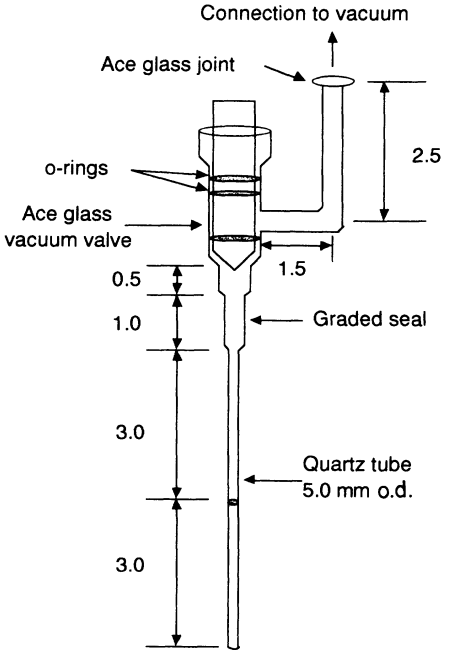

FIG. 2. Sample tube used for microwave-Hall-effect measurements. All dimensions are in inches unless otherwise noted.

A static UHV volumetric adsorption system, utilizing a turbomolecular pump (Balzers TSU 172), capable of providing a vacuum below 10^{-8} Torr in the manifold, was used to measure gas adsorption and Ar Brunauer-Emmett-Teller (B.E.T.) surface areas at liquid-nitrogen temperature. Pressures during isotherm measurements were obtained using a Baratron sensor head (MKS, model 310). Additional experimental details have been given earlier.[20] An average particle diameter was calculated from the surface area by assuming spherical particles, i.e.,

$$d(nm)=\frac{6\times10^3}{\rho A}\ , \tag{1}$$

where ρ is the density of the sample (g/cm^3) and A is the surface area (m^2/g).

Three different zinc oxides were used. An ultrahigh-purity, high-surface-area ZnO sample (1) was prepared by adding a 1-M $(NH_4)_2CO_3$ (Aesar, 99.999% purity) solution drop by drop to a 1-M $Zn(NO_3)_2$ (Aesar, 99.999% purity) solution while stirring to precipitate $ZnCO_3$. Distilled, deionized water was used. The precipitate was filtered, dried at 393 K in air for a week, then stored in a desiccator. It was decomposed to ZnO inside a quartz cell by heating under vacuum at a rate of 2 K/min to 393 K and holding for 30 min at 393 K, then heating to 533 K and holding for 30 min, and finally heating to 673 K and holding for 4 h at this maximum temperature. To establish this procedure and verify surface area measurements, a high-surface-area ZnO sample was prepared using less pure (99%) reagents.[15] Other research groups have used Na_2CO_3 instead of $(NH_4)_2CO_3$ to form zinc carbonate, but the former method can leave a Na impurity in the resulting ZnO.[21–23] Zinc carbonate does have a low solubility in ammonium solutions, so the yield of zinc carbonate is smaller than that using sodium carbonate; however, the ammonium ion can be easily decomposed by heating, thus yielding an ultrahigh-purity zinc oxide free of sodium. X-ray-diffraction analysis showed the initial presence of $ZnCO_3$ and verified that ZnO was formed after the high-temperature evacuation step.[15] No residual $ZnCO_3$ peaks could be observed. The ZnO(II) (Alfa, 99.99% purity) and ZnO(III) (Aesar, 99.9995%) samples provided powders with lower surface areas.

X-ray-diffraction patterns were obtained on a Rigaku Model 4011B3 diffractometer. These were used to verify the formation of zinc oxide and also to calculate particle sizes. Each sample was lightly pressed into a hollow aluminum holder to avoid powder movement during the rotation of the sample over 2θ values from 65° to 20° at 4°/min. The three major peaks occur at 2θ values of 36.2° ($I/I_1=100$), 34.4° ($I/I_1=56$), and 31.8° ($I/I_1=71$). For the x-ray line-broadening particle-size measurements, the samples were scanned again between 37° and 35° at 0.25°/min. The mean particle diameter d_B was calculated using the Scherrer equation

$$d_B=\frac{K_s\lambda}{B_d\cos\theta}\ , \tag{2}$$

where λ is the x-ray wavelength (Cu $K\alpha=0.154\,050$ nm), K_s is the Scherrer constant (0.89), and B_d is the angular width at half maximum intensity expressed in terms of $\Delta(2\theta)$. Warren's correction was used to account for instrumental line broadening, i.e., $B_d=(B_M^2-B_{\text{inst}}^2)^{1/2}$, where B_M is the measured angular width and B_{inst} is 0.17° at a 2θ value of 36.2°.

RESULTS

The number of charge carriers per gram can be calculated from the equation

$$N_c=\frac{\sigma}{\rho e\mu}\ (\text{g}^{-1})\ , \tag{3}$$

where σ is the conductivity in $(\Omega\,\text{cm})^{-1}$, μ is the mobility in cm^2/V s, e is the charge of an electron (1.6×10^{-19} Coulomb), and ρ is the density of zinc oxide (5.606 g/cm^3).

The microwave cavity Q factor (quality factor), i.e., the ratio of stored resonant energy to input energy, is very important in these microwave experiments as it determines the energy absorbed by the sample-cavity system as well as the electric- and magnetic-field strengths at the sample location. Q is defined as

$$Q=\frac{f}{\Delta f_{3\text{ dB}}}\ , \tag{4}$$

where f is the resonance frequency of the cavity and $\Delta f_{3\text{ dB}}$ is the frequency difference at the 3-dB position from the baseline. Two typical sets of resonance spectra measured with the cavity connected to the network analyzer are shown in Fig. 3. Curve 1 represents the resonance spectrum of the cavity detected at the inlet port (port 1) of the network analyzer, and curve 2 represents the transmitted power detected at the port orthogonal to both the electric and magnetic fields (port 2). Marker 1 gives the resonance frequency of the cavity, and the difference between markers 2 and 3 represents $\Delta f_{3\text{dB}}$. In Fig. 3(a), showing the spectra after evacuation of ZnO(I) at 673 K for 2 h, the baseline of curve 1 was at −5.5 dB, so markers 2 and 3 were positioned at −8.5 dB. Figure 3(b) shows the same set of spectra after adsorption of O_2 at 300 K.

For MHE measurements the cavity was disconnected from the network analyzer and connected to the ESR spectrometer as shown in Fig. 1, with the cavity in the normal ESR position between the dc magnetic poles. The Hall mobility is calculated from the following equation:[14,15]

$$\mu_H=\frac{2\times10^8}{B}\left[\frac{Q_0}{Q_0-Q_L}\right]\left[\frac{P_H}{P_1}\right]^{1/2}\ , \tag{5}$$

which can also be written as

$$\mu_H=\frac{2\times10^8}{B}\left[\frac{Q_0}{Q_0-Q_L}\right]\left[\frac{Y_C}{\text{RG}}\right]\ , \tag{6}$$

where μ is the mobility (cm^2/V s), B is the dc magnetic field (Gauss), and P_H/P_1 is the ratio of the Hall power (transferred to port 2) to the incident microwave power, Y_C is the signal intensity from the ESR detector after

correcting for the empty cavity signal, RG is the receiver gain of the ESR spectrometer, and Q_0 and Q_L are the unloaded and sample loaded cavity Q factors, respectively. Figure 4 shows a set of Hall signals for ZnO(I) after different treatment conditions. An ideal cavity with an empty sample holder system will give no Hall signal when an external magnetic field is applied; however, real cavities give a background Hall signal due to unavoidable mode coupling. This particular cavity with an empty quartz tube had a small background Hall signal intensity which had to be subtracted from the weaker signals; for example, it represented about $\frac{2}{3}$ of the signal in Fig. 4(c). High-mobility samples, such as a silicon semiconductor, give Hall signals so strong that the small background Hall signal can be neglected, but with zinc oxide the Hall signal is much smaller and a correction must be made for the empty cavity background signal. If it is assumed that the background signal is linearly proportional to the Q factor ratio, i.e., the ratio of the sample-loaded Q factor to the unloaded Q factor, the following relation can be obtained to get the corrected Hall signal Y_C:

$$Y_C = Y_L - Y_0 \left[\frac{Q_L}{Q_0} \right] , \tag{7}$$

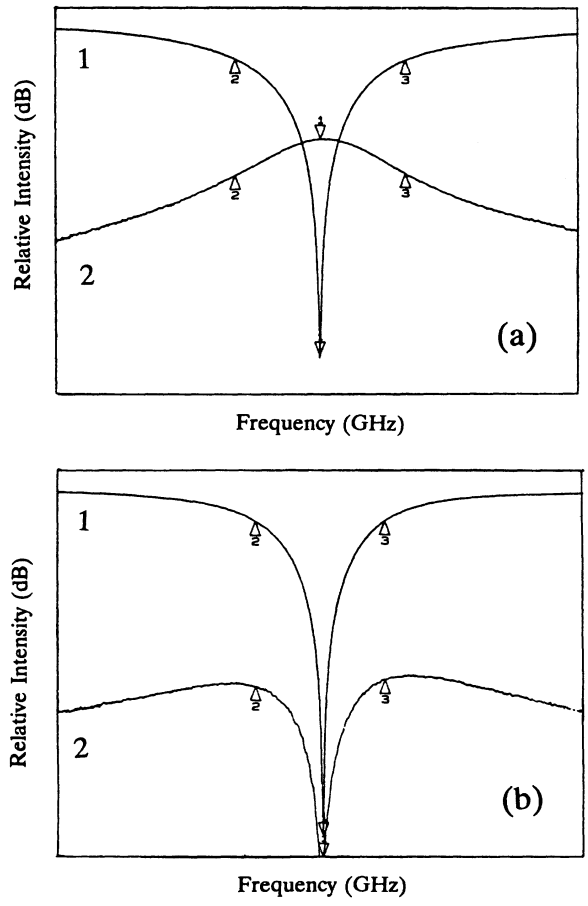

FIG. 3. Resonance spectra of ZnO(I) at 300 K using a H-P network analyzer and a bimodal TE102 rectangular cavity. Curve 1, inlet port; curve 2, orthogonal port: (a) after evacuation at 673 K for 4 h, (b) after exposure to 20 Torr O_2.

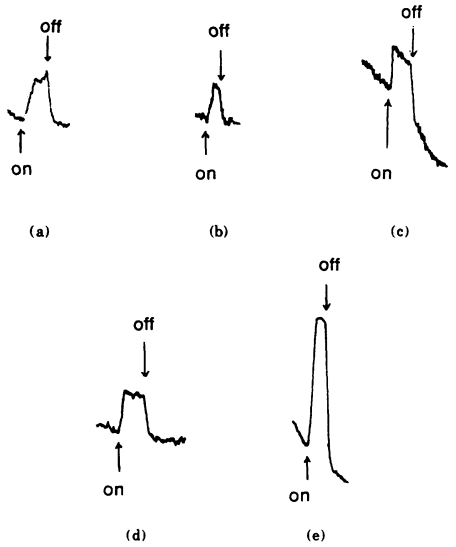

FIG. 4. MHE signal intensities of ZnO(I) at 300 K using a modified ESR spectrometer. Measurement conditions: $P=5$ mW, $MF=100$ kHz, $MA=1.0$ G, $B=5000$ G, $RG=1\times10^5$; markers indicate when the B field was turned on and off: (a) AS IS, (b) after evacuation at 673 K for 4 h, (c) after O_2 adsorption at 20 Torr, (d) after evacuation at 673 K for 2 h, (e) after next O_2 adsorption at 20 Torr. These data provide the results for sample 1 in Table II. The signal intensity of peak (b) represents about 2.5×10^{-8} mW.

where Y_L is the measured Hall signal intensity with a sample and Y_0 is the background Hall signal with the empty quartz tube.

The calculation of electrical conductivity from microwave measurements requires the use of different equations depending on which of three different conductivity regions apply.[8,15] The following equation for the low conductivity region [below 0.1 $(\Omega\,\mathrm{cm})^{-1}$] was used for zinc oxide:

$$\sigma = 2.78\times10^{-13} f \left[\frac{Q_0 - Q_L}{Q_0 - Q_L} \right] \frac{V_c}{2V_s} , \tag{8}$$

where σ is the conductivity in $(\Omega\,\mathrm{cm})^{-1}$, V_c and V_s are the cavity and sample volumes, respectively, and f is the resonance frequency (Hz) of the cavity. The Q factors and resonance frequencies were obtained with the network analyzer.

The highest conductivity values for ZnO at 300 K, which were around 0.07 $(\Omega\,\mathrm{cm})^{-1}$, were obtained after evacuation at 673 K, and the thinnest skin depth δ was consequently calculated to be 2.0 mm at 9.5 GHz (Ref. 24) using the following equation:

$$\delta = \left[\frac{2}{\omega\mu_0\sigma} \right]^{1/2} = \left[\frac{2}{2\pi f\mu_0\sigma} \right]^{1/2} , \tag{9}$$

where μ_0 is the permeability in a vacuum $=4\pi\times10^{-7}$ H/m. The particle sizes of all the ZnO samples in Table I were therefore much smaller than the skin depth. The inner radius of the quartz sample tube was 2.0 mm, so the microwave attenuation by the ZnO particles in the sam-

TABLE I. Crystallite size of ZnO samples measured by XRD and Ar B.E.T. methods.

Sample	Weight (g)	Treatment	B.E.T. area (m^2/g)	d (nm) XRD	B.E.T.
ZnO(I)[a]	0.760	Evac. 4 h at 673 K	32	19	32
(99.999%)		Evac. 2 h at 673 K (after 4 cycles)	27		
ZnO(II)	0.980	Evac. 1 h at 673 K	3.4	>80[b]	320
(Alfa, 99.99%)		Evac. 4 h at 673 K	3.4		
ZnO(III)	9.865	Evac. 1 h at 673 K	1.3×10^{-2}	>80[b]	71000
(Aesar, 99.9995%)		repeat measurement	1.8×10^{-2}		

[a]Prepared from $ZnCO_3$ precipitated from a solution of $Zn(NO_3)_2$ using $(NH_4)_2CO_3$.
[b]XRD peaks too narrow for accurate measurements.

ple bed can be neglected. In Fig. 5 the theoretical conductivity was calculated using the following assumed parameters for ZnO: $Q_0=4400$, $f_0=9.647$ GHz, $f=9.644$ GHz, and weight of 5.0 mg. The lower branch represents Eq. (8), which applies to the low conductivity region, and the upper plot represents the equation appropriate for the intermediate conductivity region:[15]

$$\sigma=1.112\times10^{-12}f\left[\frac{\Delta f}{f}\right]^2\left[\frac{Q_0Q_L}{Q_0-Q_L}\right]\frac{V_c}{2V_s}, \quad (10)$$

where Δf is the frequency difference between the empty and loaded cavity. The data are clearly accommodated extremely well by the low conductivity expression and the fit indicates that the surface effects associated with this high-surface-area ZnO do not result in unusually high overall σ values.

The surface area of zinc oxide is dependent upon the preparation method; Table I lists the B.E.T. surface areas of the three different zinc oxides used in this study.

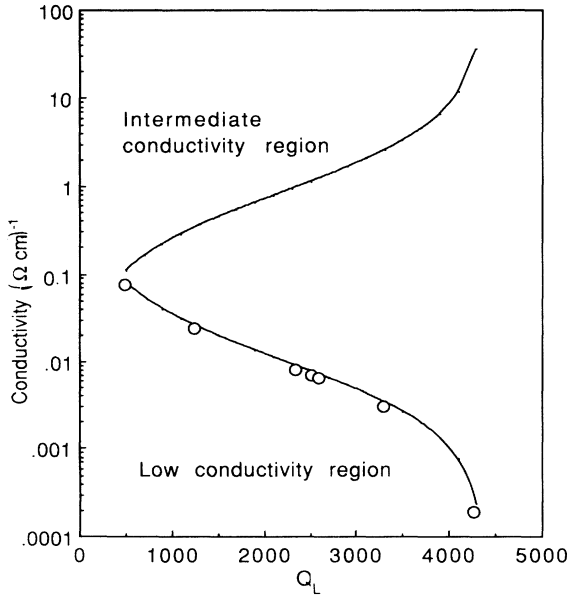

FIG. 5. Conductivity of ZnO vs the quality factor Q_L of the loaded cavity using assumed parameters (solid line) and the data obtained for ZnO(I).

ZnO(I) had a surface area of 30 ± 3 m^2/g after treatment at 673 K, but sintering occurred at 773 K which decreased the surface area to 15 m^2/g.[15] ZnO(II) and ZnO(III) had surface areas of 3.4 and 0.015 ± 0.003 m^2/g, respectively. Table I also lists average crystallite diameters calculated from x-ray-diffraction (XRD) and B.E.T. measurements. XRD line broadening is most applicable for particle sizes between 5 and 50 nm, which is the size range of ZnO(I), whereas the sharp peaks obtained for ZnO(II) and (III) provide only a minimum estimate.

Values of mobility, conductivity, and charge-carrier density for ZnO(I) after different treatment conditions were calculated using Eqs. (3)–(8), and are listed in Table II. For comparison, Table III gives literature values of mobility and conductivity for other ZnO samples.[1,7,25–32] The fresh (AS IS) sample of $ZnCO_3$ contained enough moisture to interfere with microwave measurements even though it was dried at 393 K, so its mobility and conductivity could not be compared directly with the rest of the data. In order to remove all the moisture and decompose zinc carbonate to zinc oxide, the sample was given a heat treatment at 673 K, as described in the Experiment section. Only XRD peaks for ZnO were visible after this treatment.

The Hall mobility of this ZnO powder measured after the various treatment conditions is related to changes in carrier (i.e., electron) density of the semiconductor. Measurements after oxygen adsorption at 20 Torr on ZnO(I) gave mobilities between 20 and 67 $cm^2/V\,s$ with an average value of 44 ± 19 $cm^2/V\,s$, which is about half the value of 110 ± 40 $cm^2/V\,s$ for ZnO powder reported by Trukhan[7] and is also somewhat lower than the range of values (90–200 $cm^2/V\,s$) cited for single crystals.[25–29] Evacuation of ZnO(I) at 673 K for 1–4 h lowered the mobility to 3.9 ± 0.8 $cm^2/V\,s$.

The conductivity measurements of ZnO(I) in Table II also show a significant effect of high-temperature evacuation and subsequent exposure to O_2 at 300 K. The initial 4-h evacuation at 673 K to decompose the $ZnCO_3$ gave an average conductivity of 3.8×10^{-3} $(\Omega\,cm)^{-1}$, which decreased to 5.3×10^{-4} $(\Omega\,cm)^{-1}$ following oxygen adsorption. An evacuation at 673 K for either 1 h or for 2 h following O_2 adsorption increased the electrical conductivity to 2.4×10^{-2} $(\Omega\,cm)^{-1}$ or 6.2×10^{-2} $(\Omega\,cm)^{-1}$, respectively. These values were higher than that after the initial evacuation, but readsorption of O_2 decreased the

TABLE II. The effect of oxygen adsorption at 300 K on the electrical properties of high-surface-area ZnO(I): $f_0 = 9.647\,00$ GHz and $Q_0 = 4351$. All measurements were at 300 K.

	Treatment	f (GHz)	Q_L	Signal intensity	μ (cm^2/V s)	σ (10^{-3} Ω^{-1}cm^{-1})	N_c (10^{15} e^-/g)
	AS IS ($ZnCO_3$)	9.643 40	3517	3.0	4.1	2.4	0.64
	673 K, evac. 4 h	9.644 50	3884	2.8	3.9	1.2	0.34
Sample 1	20 Torr O_2	9.644 78	4161	3.5	20	0.50	0.025
(5.3 mg)[a]	673 K, evac. 2 h	9.641 00	593	3.0	2.5	62	28
	20 Torr O_2	9.644 60	3933	10.5	67	1.0	0.017
	300 K, evac. 1 h	9.644 50	3770	9.3	42	1.5	0.040
	AS IS ($ZnCO_3$)	9.643 25	3225	3.0	2.4	3.3	1.5
	673 K, evac. 4 h	9.644 00	2581	4.0	4.4	6.4	1.6
Sample 2	20 Torr O_2	9.644 53	4104	7.0	59	0.56	0.011
(5.6 mg)[a]	673 K, evac. 1 h	9.642 70	1232	5.0	4.6	24	5.7
	20 Torr O_2	9.644 44	3987	6.0	31	0.85	0.030
	300 K, evac. 0.5 h	9.644 43	3990	5.5	27	0.84	0.035

[a]Weight of ZnO after decomposition.

conductivity back to about 9.3×10^{-4} $(\Omega\,\text{cm})^{-1}$. It is not clear why the second evacuation at 673 K following oxygen adsorption produced a higher conductivity than the first treatment, but it was principally due to an increase in electron density rather than an increase in mobility. There may have been a structural change in the zinc oxide during the second evacuation involving chemisorbed oxygen or a small residual amount of $ZnCO_3$ may have further decomposed.

Earlier studies used a conductivity cell in which the powder samples were compressed between metal electrodes,[2,3,29] but only relative changes in conductivity were reported. Amigues and Teichner also used a dc conductivity cell and reported a conductivity value of 7×10^{-2} $(\Omega\,\text{cm})^{-1}$ after heating $Zn(OH)_2$ in vacuum for 12 h at 623 K, and this value decreased to 2×10^{-3} $(\Omega\,\text{cm})^{-1}$ under 3 Torr oxygen pressure at 298 K.[1] Literature values for the conductivity of ZnO are listed in Table III, and they show that ZnO single crystals have conductivities ranging from about 0.01 to 1.0 $(\Omega\,\text{cm})^{-1}$,[1,26–28,30–32] with the minimum value of 7×10^{-3} $(\Omega\,\text{cm})^{-1}$ being obtained after heating at 980 K under 10^{-7} Torr of O_2 pressure. The range in conductivities for these ZnO single crystals indicates that defect formation can be significant during crystal growth and that the defect concentration can vary from batch to batch.[28]

The electron densities after these various pretreatments, calculated using Eq. (3) with the measured values of μ and σ, are also listed in Table II. After decomposition of $ZnCO_3$ under vacuum at 673 K for 4 h, the initial charge-carrier density was 0.34×10^{15} and 1.6×10^{15} e^-/g for samples 1 and 2, respectively. Oxygen adsorption at 300 K decreased the charge-carrier density markedly to $1.8\pm0.7\times10^{13}$ e^-/g. An electron density of 3×10^{14} e^-/g has been reported for a ZnO single crystal grown from the vapor phase.[28] For sample 1, a 2-h evacuation at 673 K decreased the mobility to 2.5 cm^2/V s, but increased the conductivity to 6.2×10^{-2} $(\Omega\,\text{cm})^{-1}$, primarily because of the marked increase in electron density to 28×10^{15} e^-/g. Irreversible oxygen readsorption at 300 K ($\sim230\times10^{15}$ molecules/g) reproduced the same effect as the initial adsorption and very similar N_c values were obtained on both samples. A 1-h evacuation at 300 K changed the sample properties only slightly, which indicated that the oxygen was essentially irreversibly chemisorbed. A combined MHE-ESR study has shown that this chemisorbed oxygen can not only interact with conduction electrons to form O_2^- species, thereby decreasing

TABLE III. Literature values for electron mobility and conductivity of ZnO at 300 K.

Sample	Treatment	Mobility (cm^2/V s)	Conductivity $(\Omega\,\text{cm})^{-1}$	Ref.
Single crystal		90–140		25
Single crystal	heating at 980 K in $P_{O_2}=10^{-7}$ Torr	130–200	~0.007	26
Single crystal		150	0.1–1.0	27
Single crystal	grown from vapor phase	180	0.01–3.0	28
	extremely high purity and crystallinity	200		29
Single crystal	grown from vapor phase		0.13	30
Single crystal	grown from vapor phase		~0.01	31
Crystalline			1.0	32
Powder		110±40		7
Powder	decomposition of $Zn(OH)_2$ at 623 K		~0.07	1
	O_2 adsorption at 298 K		~0.002	

TABLE IV. Electrical properties of ZnO(II) and ZnO(III): $f_0=9.647\,00$ GHz, $Q_0=4351$ for ZnO(II); $f_0=9.645\,41$ GHz and $Q_0=4271$ for ZnO(III); O_2 adsorption at 300 K.

	Treatment	f (GHz)	Q_L	Scale reading	μ ($cm^2/V\,s$)	σ ($10^{-3}\ \Omega^{-1}\,cm^{-1}$)	N_c ($10^{15}\ g^{-1}$)
ZnO(II) (6.0 mg)	AS IS	9.644 95	3707	4.5	13	1.5	0.13
	673 K evac. 2 h	9.645 08	3693	3.0	4.6	1.5	0.37
	20 Torr O_2	9.645 00	3878	3.5	9.4	1.1	0.13
	673 K evac. 2 h	9.644 88	3493	3.0	4.0	2.1	0.59
	20 Torr O_2	9.644 95	3810	4.5	15	1.2	0.093
ZnO(III) (4.8 mg)	AS IS	9.644 08	2511	7.5	11	6.4	0.63
	673 K evac. 2 h	9.644 78	2524	7.0	10	6.4	0.68
	20 Torr O_2	9.644 40	2670	5.0	7	5.5	0.87
	673 K evac. 2 h	9.643 75	2428	10.0	15	7.0	0.50
	20 Torr O_2	9.643 80	2506	11.0	18	6.5	0.40

free electron density, but it can also interact with the unpaired electron at singly ionized oxygen vacancies to form additional O_2^- species and it can remove oxygen vacancies completely by a bulk reoxidation process.[16] Consequently, the chemistry can be complex. The results in Table II show small differences in measured electrical properties for two different ZnO samples using slightly different experimental procedures, but the change in each property has the same trend for similar experimental sequences.

A ZnO(II) sample with a lower surface area of 3.4 m^2/g showed the same trends as the higher-surface-area ZnO(I) but the variations in electrical properties were smaller, as shown in Table IV. This is undoubtedly due to the smaller surface-to-volume (S/V) ratio of ZnO(II). A sample of ZnO(III) with the lowest surface area of ~ 0.015 m^2/g was also examined, and the results after pretreatments comparable to those used for the other two types of ZnO are also listed in Table IV so that the particle-size effect on electrical properties can be further determined. The carrier density of ZnO(III) also increased after an evacuation at 673 K and decreased after adsorption of oxygen at 300 K, but the relative changes were much smaller than those obtained with ZnO(I). The electron density of ZnO(III) was much more insensitive to pretreatment. Both the mobilities and conductivities of ZnO(III) were consistently higher than comparable values of ZnO(II); consequently, electron densities for ZnO(II) and ZnO(III) were about the same.

The effects of sequential CO and O_2 adsorption on ZnO(I) are shown in Table V. After the measurements listed in Table II, sample I was evacuated at 673 K which increased electron density back to a high level of 3.1×10^{16} e^-/g. CO adsorption (1.0×10^{17} molecule/g) at 300 K was completely reversible and had no significant effect on the electrical properties of high-temperature evacuated ZnO. This is consistent with the fact that CO adsorption on ZnO at low temperature is weak and reversible.[15,16,33–35] After evacuation at 300 K, oxygen was adsorbed, which decreased the carrier density as expected although not quite as much as before.

After reevacuation at 673 K, which again increased N_c, O_2 was adsorbed and then evacuated at 300 K leaving the ZnO surface covered with strongly adsorbed oxygen. Adsorption of CO onto this surface at 300 K increased the electron density almost two orders of magnitude and increased μ more than tenfold, thus indicating that CO can react with adsorbed oxygen at 300 K in such a way as to release electrons to the zinc oxide. Such a reaction has been recently reported by Chiorino, Ghiotti, and Boccuzzi.[18] Also, Hotan, Göpel, and Haul[30] have measured the dc conductivity of a ZnO single crystal which was an-

TABLE V. Electrical properties of ZnO(I) after adsorption of oxygen and carbon monoxide at 300 K: 5.3 mg, $f_0=9.647\,00$ GHz and $Q_0=4351$. Experiments were continued with sample 1 from Table II.

Treatment	f (GHz)	Q_L	Scale reading	μ ($cm^2/V\,s$)	σ ($10^{-3}\ \Omega^{-1}\,cm^{-1}$)	N_c ($10^{15}\ g^{-1}$)
673 K, evac. 2 h	9.638 73	548	3.0	2.5	68	31
2.0 Torr CO	9.641 50	652	3.0	2.5	56	25
20 Torr CO	9.641 01	606	3.0	2.5	61	26
300 K, evac. 1 h; 20 Torr O_2	9.644 30	3682	5.8	19	1.8	0.11
673 K, evac. 2 h	9.641 62	602	3.0	2.5	61	28
2.0 Torr O_2	9.644 35	3484	11.0	36	2.4	0.076
20 Torr O_2	9.644 48	3728	12.0	55	1.6	0.033
300 K, evac. 1 h	9.644 22	3585	6.8	21	2.1	0.11
2.0 Torr CO	9.643 45	1929	3.0	2.7	12	5.1
20 Torr CO	9.642 65	1391	3.0	2.6	21	9.0

TABLE VI. Electrical properties of ZnO(I) after the adsorption of oxygen and hydrogen at 300 K: 5.3 mg, $f_0 = 9.647\,00$ GHz and $Q_0 = 4351$. Experiments were continued with sample 1 from Table V.

Treatment	f (GHz)	Q_L	Scale reading	μ ($cm^2/V\,s$)	σ ($10^{-3}\ \Omega^{-1}\,cm^{-1}$)	N_c ($10^{15}\ g^{-1}$)
673 K, evac. 2 h	9.641 79	773	3.0	2.5	46	20
2.0 Torr H_2	9.642 31	860	3.0	2.5	40	18
20 Torr H_2	9.641 88	890	3.0	2.5	38	17
300 K, evac. 1 h; 20 Torr O_2	9.644 27	3565	5.0	13	2.2	0.18
673 K, evac. 2 h	9.643 00	721	3.0	2.5	50	22
20 Torr O_2	9.644 48	3827	5.0	18	1.3	0.081
300 K, evac. 1 h; 20 Torr H_2	9.644 45	3745	5.0	16	1.6	0.11

nealed under an oxygen pressure of 1×10^{-4} Pa and then exposed to CO at 298 K. They found that σ increased and suggested that a chemical reduction of the surface occurred which donated charge to the ZnO conduction band. This result shows that the net effect of CO adsorption on the electron density of ZnO is extremely dependent on the state of the surface.

Measurements of the electrical properties of this ZnO(I) sample were also made after sequential hydrogen and oxygen adsorption, with the results given in Table VI. After evacuation at 673 K, irreversible hydrogen adsorption was low (19×10^{17} molecule H_2/g) and had only a very small effect on the electrical properties. Hydrogen adsorbed at 300 K on a surface precovered with oxygen also caused no significant change in any electrical property. Unlike CO, hydrogen does not interact with adsorbed oxygen at 300 K to significantly affect the electrical properties of zinc oxide.

Sequential adsorption of CO_2 and O_2 gave the interesting results shown in Table VII. Irreversible CO_2 adsorption (95 μmol/g) at 300 K after evacuation at 673 K was large (570×10^{17} molecule/g) and decreased the carrier density from 20×10^{14} to $1.5\times10^{14}\ e^-$/g, thus indicating that adsorbed CO_2 significantly reduced conduction electron density, but less than chemisorbed O_2. This low ratio of electron transfer per adsorbed CO_2 molecule is consistent with previous work.[30] CO_2 adsorbed on an oxygen-precovered surface at 300 K also decreased the charge-carrier density. dc conductivity measurements with a ZnO single crystal had previously indicated a decrease in conductivity after exposure to CO_2.[30] Two explanations for the decrease in N_c for CO_2 adsorption on the oxygen-covered surface are either CO_2 adsorption on sites not available to O_2 or CO_2 interaction with chemisorbed oxygen in a manner that withdraws more conduction electrons from the zinc oxide. The chemistry associated with these interactions is also complex and is discussed in greater detail elsewhere.[15,16]

Finally, upon the completion of all of these runs, the sample of ZnO in Table VII was heated at 673 K for 2 h under 200 Torr oxygen to produce the most stoichiometric form of ZnO(I). This state of ZnO with the lowest defect density had a high mobility of 46 $cm^2/V\,s$, a low conductivity of $0.6\times10^{-3}\ (\Omega\,cm)^{-1}$, and a low electron density of $1.5\times10^{-13}\ e^-$/g.

DISCUSSION

Zinc oxide is an n-type semiconductor whose electrical properties can depend on the surface-to-volume (S/V) ratio and treatment conditions. Consistent with previous work, this study has shown that evacuation at 673 K increases the conductivity, decreases the mobility, and increases the carrier density of ZnO. However, the importance of the present study is that microwave techniques were employed to allow the characterization of ZnO powders, thus providing the opportunity to examine the influence of the surface region on absolute values of overall electrical properties. The oxygen vacancies generated by high-temperature evacuation are mostly near the surface because they can be almost completely removed by O_2 chemisorption at 300 K. The defects present in ZnO after such a treatment are not yet completely understood, but the formation of oxygen vacancies V_0 is known and there is also evidence of interstitial zinc atoms Zn_i.[26,36,37] Göpel and Lampe report the first

TABLE VII. Electrical properties of ZnO(I) after adsorption of oxygen and carbon dioxide at 300 K: 5.3 mg, $f_0 = 9.647\,00$ GHz and $Q_0 = 4351$. Experiments were continued with sample 1 from Table VI.

Treatment	f (GHz)	Q_L	Scale reading	μ ($cm^2/V\,s$)	σ ($10^{-3}\ \Omega^{-1}\,cm^{-1}$)	N_c ($10^{15}\ g^{-1}$)
673 K, evac. 2 h	9.639 76	594	4.0	3.4	62	20
20 Torr CO_2	9.643 38	2472	4.5	5.7	7.5	1.5
673 K, evac. 2 h	9.639 63	535	4.0	3.4	70	23
20 Torr O_2; evac. 1 h at 300 K	9.643 85	3181	4.0	6.5	3.6	0.62
20 Torr CO_2	9.644 00	3748	4.0	11	1.6	0.17
673 K, 2 h under 200 Torr O_2	9.644 18	4095	5.8	46	0.6	0.015

ionization level for oxygen vacancies, i.e., $(V_0)^{=} \rightarrow (V_0^+)^- + e^-$, to be 0.04 eV, and the second ionization level, i.e., $(V_0^+)^- \rightarrow (V_0^{2+})^0 + e^-$, to be 0.2–0.4 eV.[26] Consequently, it should be easy to create surface $(V_0^+)^-$ sites, but not $(V_0^{2+})^0$ defects. (The superscript sign within the parentheses represents the net charge at the defect site and the sign outside the parentheses gives the number of electrons associated with the site.) Another source of conduction electrons could be interstitial Zn^+ or Zn^{2+} ions, but it is not clear which interstitial zinc ion would be favored during evacuation.[38–40]

Mobility is a parameter describing the ease of carrier motion in an applied electric field. For zinc oxide, mobility is determined by the scattering mechanisms for conduction electrons.[41,42] Scattering mechanisms include lattice scattering with optical, acoustical, and piezoelectric modes and defect scattering from ionized and neutral defects in the lattice.[28,42–44] Hagemark and Chacka[42] and Li and Hagemark[43] calculated the contribution from each electron scattering mode to the theoretical mobilities for doped ZnO single crystals and concluded that lattice scattering is the dominant mechanism at room temperature, whereas defect scattering dominates only at very low temperature (below 50 K). These conclusions may be valid for large single crystals, but as particle size decreases the electron mobility will be increasingly determined by surface conditions. The mobility of ZnO(I) decreased by an order of magnitude after evacuation at 673 K and significantly increased following adsorption of O_2. Because the bulk structure of ZnO should not be changed significantly by O_2 adsorption at 300 K, lattice scattering should be unchanged. Consequently, the most probable explanation for the measured mobility changes is defect-caused scattering near the surface, which reduces electron mobilities for small particles with high S/V ratios. The mobility of a semiconductor is related to the mean free path of the charge carriers. For ZnO particle sizes much larger than the mean free path of conduction electrons, the condition of the surface has little effect on the mean free path because the number of scattering interactions in the bulk is much greater than at the surface. However, if the particle size becomes small enough to approach the mean free path, the electron motion will be limited by scattering in the surface region, thereby reducing the mobility. Oxygen removal during ZnO evacuation at 673 K is facilitated by higher surface areas, which resulted in a markedly higher concentration of oxygen vacancies, $(V_0)^{=}$, for ZnO(I). The higher surface defect concentration decreases the mobility and increases the carrier density to a greater extent than with lower surface area ZnO. The measured increases in electron density do not explain the measured mobility decreases at these low electron densities because the mean free path for electron-electron scattering is at least ten times greater than that for lattice scattering.[45] Thus we conclude that oxygen vacancies near the surface act as defect scattering centers for the electrons and decrease the mobility. Oxygen adsorption removes these oxygen vacancies and restores the mobility to a value near that for stoichiometric ZnO.

Another possible explanation for the mobility change in ZnO powder is the presence of surface electron trapping sites that restrict the motion of electrons.[46] Such trapping sites would interact with an electron for a certain period of time before releasing it, thereby decreasing electron motion. However, if the holding time at the trapping site is comparable to or longer than the electron collision time τ, the trapping centers would lower the measured value of electron density N_e rather than the measured value of mobility μ. Therefore, an increase in defect scattering is the preferred explanation at this time for the mobility decrease.

The mobility of electrons is related to the mean free path $\bar{l}$, which can be calculated from a kinetic model similar to that for gases.[24,47] The mean thermal velocity of electrons inside a crystal v_{th} is given by the formula

$$v_{\text{th}}(\text{cm/s}) = \sqrt{3kT/m^*} , \tag{11}$$

where k is Boltzmann's constant (1.38×10^{-16} erg/K), T is the temperature (K), m^* is the effective mass (g), which must be used instead of the free-electron mass m_0 (9.1×10^{-28} g). The mean free path is obtained by the relationship

$$\bar{l} = \tau v_{\text{th}} , \tag{12}$$

where τ is the collision time, which can be expressed in terms of the measured mobility as

$$\tau = \frac{m^* \mu}{e} , \tag{13}$$

where e is the charge of an electron (1.6×10^{-19} Coulomb) and μ is the mobility ($\text{cm}^2/\text{V s}$). Consequently, from these three equations the mean free path can be represented as

$$\bar{l} = \frac{\mu}{e}(3m^* kT)^{1/2} . \tag{14}$$

Using the literature value of $m^*/m_0 = 0.27$ for electrons in ZnO (Refs. 29 and 48) and the largest literature value of $\mu = 200$ $\text{cm}^2/\text{V s}$,[29] the longest mean free path for ZnO at 300 K is calculated to be about 7 nm. The XRD and B.E.T. results for ZnO(I) indicate average particle sizes of 20–30 nm after evacuation at 673 K, as listed in Table I; thus the radii of these particles (10–15 nm) are comparable to the mean free path, which provides a situation where electron motion could be strongly affected by the surface region of this high-surface-area powder.

The effect of particle size on the electrical properties is demonstrated by the three ZnO samples with different particle sizes. The mobility, conductivity, and carrier density for these ZnO samples are plotted against the S/V ratio in Figs. 6–8. Here μ, σ, and N are the respective values after evacuation at 673 K, while μ_0, σ_0, and N_0 represent the values after subsequent O_2 adsorption at 300 K. The ranges of mobility and conductivity for ZnO single crystals are taken from Table III, and typically only the lowest of these reported values are near those measured for these powders. However, the range of electron density, particularly that after evacuation, falls within that reported previously for ZnO single crystals. Figure 9 shows the changes in the relative values of mo-

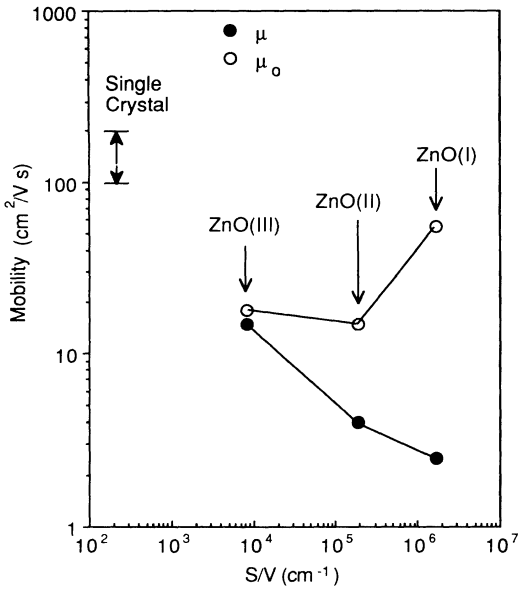

FIG. 6. Mobility at 300 K vs the surface-to-volume ratio for three different ZnO powders; μ is the value after evacuation at 673 K and μ_0 is that after O_2 adsorption at 300 K. The mobility range for a single crystal is derived from Table III.

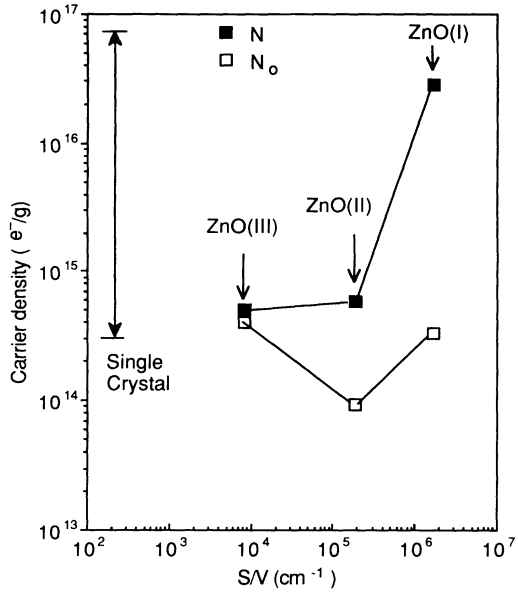

FIG. 8. Electron density at 300 K vs the S/V ratio for three different ZnO powders: N is the value after evacuation at 673 K and N_0 is that after O_2 adsorption at 300 K. The range of electron density for a single crystal is based on different doping concentrations (Ref. 26).

bility, conductivity, and carrier density after exposure to O_2 as a function of the S/V ratio for the three zinc-oxide samples. For very small S/V ratios, i.e., for very large particles, the electrical properties are relatively insensitive to pretreatment. However, at much higher S/V ratios large changes occur, especially in regard to electron density. The consistent trends among all these parameters provide strong evidence that oxygen vacancies formed in the ZnO surface region play an important role in ZnO electrical properties. Since these microwave techniques measure overall electrical properties, which are determined by both bulk and surface contributions, the comparisons in Fig. 9 show that these methods become surface sensitive when the S/V ratio becomes very large.

Previous measurements using a conductivity cell have

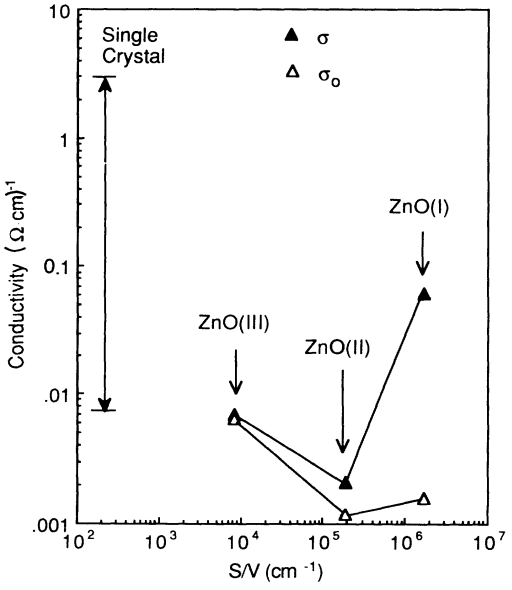

FIG. 7. Conductivity at 300 K vs the S/V ratio for three different ZnO powders: σ is the value after evacuation at 673 K and σ_0 is that after O_2 adsorption at 300 K. The conductivity range for a single crystal is obtained from Table III.

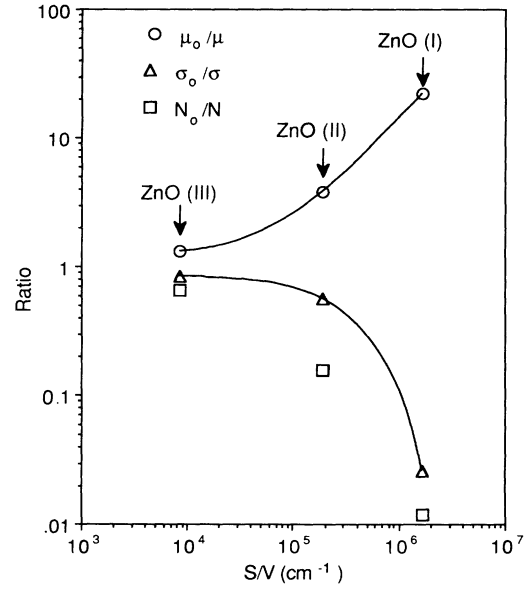

FIG. 9. Relative values of mobility, conductivity, and electron density for ZnO vs the S/V ratio. The terms μ, σ, and N are the values after evacuation at 673 K and μ_0, σ_0, and N_0 are those after O_2 adsorption at 300 K.

shown that high-temperature evacuation increases conductivity and oxygen adsorption decreases it. Two types of chemisorbed oxygen on zinc oxide at room temperature have been proposed—one is an adsorbed O^- ion formed by a reaction with conduction electrons[2,3,49,50] and the other is an O_2^- radical.[51,54] Both may even be formed simultaneously;[55] however, ESR and Fourier-transform-infrared (FTIR) spectra support O_2^- as the predominant adsorbed species on ZnO surfaces.[15,16] The matching of Fermi energy levels can be used to explain charge transfer for chemisorption of gases on semiconductors,[56] and the decrease in the charge-carrier density of ZnO during the adsorption of oxygen results from the transfer of conduction electrons from ZnO to the oxygen to form surface O_2^- species.[36] This reaction continues until equilibrium is attained between adsorption and desorption.

Variations in electrical conductivity are often considered to be due only to changes in the concentration of charge carriers at low carrier densities, i.e., the mobility is assumed to be constant.[57] The results in this study clearly show that the mobility can change by an order of magnitude or more after different treatment conditions, even at relatively low electron densities of $10^{13}-10^{16}$ e^-/g; therefore, this is a dangerous assumption. To better understand the influence of surface chemistry on electrical properties of small particles, mobility as well as conductivity must be measured.

SUMMARY

This application of a microwave-Hall-effect technique has observed changes in electrical properties of powder samples under controlled treatment conditions. Charge-carrier mobility has been shown to be a critical parameter for a better understanding of the role of surface chemistry on electrical properties of small particles. Mobility cannot be assumed constant, even at low electron densities, because 20- to 30-fold increases can occur during O_2 chemisorption at only 300 K following a high-temperature evacuation of a high-surface-area ZnO. The mobility of a high-surface-area ZnO decreased more than an order of magnitude after evacuation at 673 K, and this is attributed to the creation of oxygen vacancies in the surface region. These oxygen vacancies act as defect scattering centers for electrons, thus greatly decreasing their mobility. Bulk lattice scattering of electrons is the dominant mechanism in large ZnO particles (particle radius $\gg$ electron mean free path), but as the particle size approaches the electron mean free path, surface defect scattering begins to dominate. Chemisorbed oxygen removes these surface defect centers.

The measured conductivities of ZnO samples after O_2 exposure, i.e., at near stoichiometric Zn/O ratios, were around $10^{-2}-10^{-3}$ $(\Omega\,\mathrm{cm})^{-1}$, which is at the low end of the range of values reported for ZnO single crystals. This substantiates the statement that even carefully grown ZnO single crystals can contain substantial concentrations of bulk defects. As the S/V ratio increases, i.e., as the particle size becomes smaller, oxygen removal and adsorption is facilitated and the electrical properties can be changed significantly by heat treatment and subsequent oxygen adsorption. After evacuation at 673 K, the electron density of ZnO(I) increased 1000-fold from a value near 2×10^{-13} e^-/g, but it could be returned to its initial value by the irreversible adsorption of O_2 at 300 K. CO adsorption had little effect on an evacuated surface, but CO adsorbed on an oxygen-precovered ZnO surface increased the electron number density significantly, thus indicating that the CO reacted with the chemisorbed oxygen and allowed electrons to be donated to the conduction band. In contrast, H_2 adsorption had no effect on the electrical properties of the zinc oxide. The adsorption of CO_2 lowered the electron density in both the high-temperature evacuated sample and the oxygen-precovered zinc oxide. This implies that some of the adsorption sites for CO_2 are different from those for O_2. This study has demonstrated that microwave-Hall-effect and conductivity measurements can be used not only to characterize powders, but also to examine the influence of the surface on electrical properties.

ACKNOWLEDGMENTS

This research was partially supported by the National Science Foundation (NSF) under Contract No. CBT85-14723, and by the Florida Power & Light Company. Funding for a NSF Equipment Grant (CBT-8505572) is also gratefully acknowledged.

*Author to whom correspondence should be sent.

[1]P. Amigues and S. J. Teichner, Discuss. Faraday Soc. **41**, 362 (1966).
[2]R. Glemza and R. J. Kokes, J. Phys. Chem. **69**, 3254 (1965).
[3]R. Glemza and R. J. Kokes, J. Phys. Chem. **66**, 566 (1962).
[4]H. Chon and C. D. Prater, Discuss. Faraday Soc. **41**, 380 (1966).
[5]H. Chon and J. Pajares, J. Catal. **14**, 257 (1969).
[6]R. I. Holliday and M. Pitt, J. Catal. **17**, 121 (1970).
[7]E. M. Trukhan, Prib. Tekh. Eksp. **4**, 198 (1965) [Instrum. Exp. Tech. (USSR) **4**, 947 (1965)].
[8]N. P. Ong, Ph.D. thesis, The University of California, Berkeley, 1976.
[9]N. P. Ong, W. Bauhofer, and C. Wei, Rev. Sci. Instrum. **52**, 1367 (1981).
[10]D. D. Eley and R. Pethig, Discuss. Faraday Soc. **51**, 164 (1971).
[11]D. D. Eley and N. C. Lockhart, J. Phys. E **16**, 47 (1983).
[12]M. M. Sayed and C. R. Westgate, Rev. Sci. Instrum. **46**, 1074 (1975).
[13]M. M. Sayed and C. R. Westgate, Rev. Sci. Instrum. **46**, 1080 (1975).
[14]B. K. Na, S. L. Kelly, M. A. Vannice, and A. B. Walters, Meas. Sci. Technol. **2**, 770 (1991).
[15]B. K. Na, Ph.D. thesis, The Pennsylvania State University, 1991.

[16]B. K. Na, A. B. Walters, and M. A. Vanice (unpublished).
[17]T. Inoue, T. Iizuka, and K. Tanabe, Bull. Chem. Soc. Jpn. **60**, 2663 (1987).
[18]A. Chiorino, G. Ghiotti, and F. Boccuzzi, Vacuum **41**, 16 (1990).
[19]V. M. Allen, W. E. Jones, and P. D. Pacey, Surf. Sci. **220**, 193 (1989).
[20]A. A. Chen, M. A. Vannice, and J. Phillips, J. Phys. Chem. **91**, 6257 (1987).
[21]R. G. Herman, K. Klier, G. W. Simmons, B. P. Finn, and J. B. Bulko, J. Catal. **56**, 407 (1979).
[22]M. Bowker, H. Houghton, K. C. Waugh, T. Giddings, and M. Green, J. Catal. **84**, 252 (1983).
[23]D. L. Roberts and G. L. Griffin, J. Catal. **110**, 117 (1988).
[24]L. Solymar and D. Walsh, *Lectures on the Electrical Properties of Materials,* 3rd ed. (Oxford University, New York, 1984).
[25]H. Rupprecht, J. Phys. Chem. **6**, 144 (1958).
[26]W. Göpel and U. Lampe, Phys. Rev. B **22**, 6447 (1980).
[27]J. Lagowski, H. C. Gatos, R. Holmstrom, and C. L. Balestra, Surf. Sci. **76**, L575 (1978).
[28]A. R. Hutson, Phys. Rev. **108**, 222 (1957).
[29]S. M. Sze, *Physics of Semiconductor Devices* (Wiley-Interscience, New York, 1969).
[30]W. Hotan, W. Göpel, and R. Haul, Surf. Sci. **83**, 162 (1979).
[31]U. Schwing and B. Hoffmann, in *Grain Boundary Phenomena in Electronic Ceramics,* edited by L. M. Levinson (American Ceramic Society, Columbus, OH, 1981), Vol. 1, p. 383.
[32]W. C. Richmond and M. A. Seitz, in *Grain Boundary Phenomena in Electronic Ceramics* (Ref. 31), p. 425.
[33]R. R. Gay, M. H. Nodine, V. E. Henrich, H. J. Zeiger, and E. I. Solomon, J. Am. Chem. Soc. **102**, 6752 (1980).
[34]W. H. Cheng and H. H. Kung, Surf. Sci. **122**, 21 (1982).
[35]M. R. McClellan, M. Trenary, N. D. Shinn, M. J. Sayers, K. L. D'Amico, E. I. Solomon, and F. R. McFeely, J. Chem. Phys. **74**, 4726 (1981).
[36]T. I. Barry, F. S. Stone, Proc. R. Soc. London, Ser. A **255**, 124 (1960).
[37]A. Pöppel and G. Völkel, Phys. Status Solidi A **115**, 247 (1989).
[38]J. O. Cope and I. D. Campbell, J. Chem. Soc. Faraday Trans. I **69**, 1 (1973).
[39]V. Bolis, B. Fubini, E. Giamello, and A. Reller, J. Chem. Soc. Faraday Trans. I **85**, 855 (1989).
[40]M. Watanabe, Jpn. J. Appl. Phys. **19**, 1853 (1980).
[41]R. F. Pierret, *Modular Series on Solid State Devices; Vol. 1, Semiconductor Fundamentals* (Addison-Wesley, Reading, MA, 1983).
[42]K. I. Hagemark and L. C. Chacka, J. Solid State Chem. **15**, 261 (1975).
[43]P. W. Li and K. I. Hagemark, J. Solid State Chem. **12**, 371 (1975).
[44]J. D. Zook, Phys. Rev. **136**, A869 (1964).
[45]C. Kittel, *Introduction to Solid State Physics,* 6th ed. (Wiley, New York, 1986).
[46]K. C. Kao and W. Hwang, *Electrical Transport in Solids* (Pergamon, Oxford, 1981).
[47]K. W. Böer, *Survey of Semiconductors Physics* (Van Nostrand Reinhold, New York, 1990).
[48]D. L. Rode, in *Semiconductors and Semimetals: Vol. 10, Transport Phenomena,* edited by R. K. Willardson and A. C. Beer (Academic, New York, 1975), p. 1.
[49]R. J. Kokes, J. Phys. Chem. **66**, 99 (1962).
[50]T. I. Barry and K. Klier, Discuss. Faraday Soc. **31**, 219 (1961).
[51]A. J. Tench and T. Lawson, Chem. Phys. Lett. **8**, 177 (1971).
[52]J. H. Lunsford and J. P. Jayne, J. Chem. Phys. **44**, 1487 (1966).
[53]R. D. Iyengar, V. V. Subba Rao, and A. C. Zettlemoyer, Surf. Sci. **13**, 251 (1969).
[54]F. Boccuzzi, G. Ghiotti, and A. Chiorino, J. Chem. Soc. Faraday Trans. 2 **79**, 1779 (1983).
[55]J. H. C. van Hooff, J. Catal. **11**, 277 (1968).
[56]F. S. Stone, in *Chemistry of the Solid State,* edited by W. E. Garner (Butterworths, London, 1955), p. 367.
[57]B. M. Arghiropoulos and S. J. Teichner, J. Catal. **3**, 477 (1964).

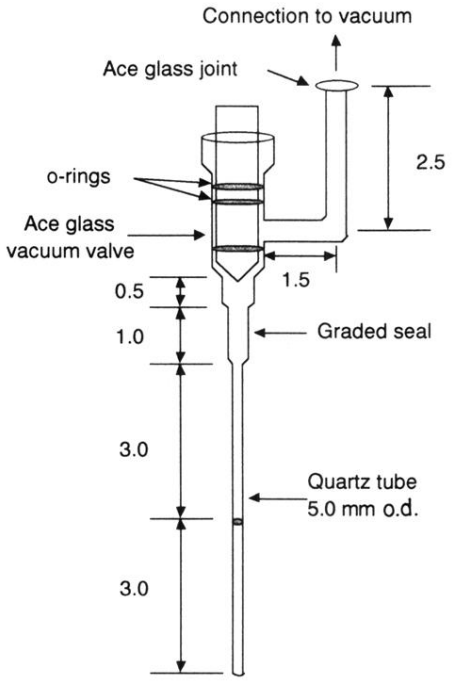

FIG. 2. Sample tube used for microwave-Hall-effect measurements. All dimensions are in inches unless otherwise noted.